https://doi.org/10.15407/ujpe69.11.774

V. BAIRATHI (for the STAR Collaboration)

Instituto de Alta Investigación, Universidad de Tarapacá
(Casilla 7D, Arica 1000000, Chile; e-mail: vipul.bairathi@gmail.com)

COLLECTIVE PROPERTIES OF THE NUCLEAR MATTER FROM THE STAR EXPERIMENT AT RHIC[1]

The study of a collective flow offers valuable insights into the dynamics and properties of the Quark-Gluon Plasma (QGP) medium produced in heavy-ion collisions. The directed flow (v_1) slope (dv_1/dy) of protons at mid-rapidity is expected to be sensitive to the first-order phase transition. The scaling of the elliptic flow (v_2) with the number of constituent quarks (NCQ) can be regarded as a signature of the QGP formation. The triangular flow (v_3) typically originates from fluctuations and can offer constraints on the initial state geometry and fluctuations. The STAR experiment at RHIC has gathered data across a wide range of energies and systems. The second phase of the Beam Energy Scan program, including a Fixed-Target mode is done to collect high-statistics data on $Au + Au$ collisions in the high baryon density region of the Quantum Chromodynamics (QCD) phase diagram. In these proceedings, we discuss selected results on the collective properties of the nuclear matter from the STAR experiment at RHIC.

K e y w o r d s: heavy-ion collisions, quark-gluon plasma, collective flow.

1. Introduction

Quantum Chromodynamics suggests a transition from confined hadronic matter to a state of deconfined partonic matter known as the Quark-Gluon Plasma (QGP) at high temperatures and energy densities [1]. Under these extreme conditiozns, hadrons break down into constituent quarks, and the strong interaction becomes the dominating force. High-energy heavy-ion collisions have been conducted by various experiments at the Brookhaven National Laboratory (BNL) and the European Organization for Nuclear Research (CERN) to explore this new state of matter. Experimental results from the Relativistic Heavy Ion Collider (RHIC) and Large Hadron Collider (LHC) at their top energies indicate the formation of a new state of matter with partonic degrees of freedom. Figure 1 shows a schematic layout of the QCD phase diagram between temperature (T) and baryon chemical potential ($\mu_{\rm B}$) with various expected phases of the matter [2].

Lattice QCD calculations indicate that the phase transition in the low $\mu_{\rm B}$ region is a smooth crossover at T_c of about 150 MeV [3]. In the high $\mu_{\rm B}$ region of the QCD phase diagram, the transition is expected to be first order ending at a critical end point as one progresses to lower $\mu_{\rm B}$ [3]. An experimental way to characterize the QCD phase diagram is to scan T and $\mu_{\rm B}$ by varying the beam energy. Heavy-ion collision experiments aiming at this high $\mu_{\rm B}$ region are currently being pursued at NA61/SHINE, SIS18/HADES, and RHIC. Various new experimental facilities at FAIR, NICA, and J-PARC are planned for future studies. The STAR experiment at RHIC has been actively working on the beam energy scan (BES) program to explore the QCD phase diagram especially for the investigation of the first-order phase transition, as well as signatures from the critical end point. The first phase of the BES program was successfully conducted in the beam energy range of $\sqrt{s_{NN}} = 7.7$ to 62.4 GeV, corresponding to the $\mu_{\rm B}$ between 20 and 420 MeV. The second phase including the Fixed-Target (FXT) mode has completed data taking with high statistics data for $\rm Au + Au$ collisions with $\sqrt{s_{NN}} = 3.0$ to 19.6 GeV, corresponding

Citation: Bairathi V. (for the STAR Collaboration). Collective properties of the nuclear matter from the STAR experiment at RHIC. *Ukr. J. Phys.* **69**, No. 11, 774 (2024). https://doi.org/10.15407/ujpe69.11.774.

[1] This work is based on the results presented at the 2024 "New Trends in High-Energy and Low-x Physics" Conference.

to μ_B = range 200 to 720 MeV, to explore the QCD phase diagram [4].

In this proceedings, we will present selected results of collective flow from Au + Au collisions at the top RHIC energy ($\sqrt{s_{NN}}$ = 200 GeV) and the BES program ($\sqrt{s_{NN}}$ = 3.0 to 27 GeV). Additionally, results from the data collected for the deformed nuclei, such as Isobars (Ru + Ru and Zr + Zr) and U + U collisions will be discussed. The experimental results will be compared with model calculations to better understand the underlying physics mechanisms in heavy-ion collisions.

2. STAR Experiment at RHIC

RHIC is a highly versatile collider, capable of colliding various nuclear species (U, Au, Ru, Zr, Cu, Al, O, ^{3}He and d) and protons, at energies between $\sqrt{s_{NN}}$ = 7.7 GeV and 200 GeV in collider mode, and from 3.0 to 7.7 GeV in fixed-target mode.

The Solenoidal Tracker at RHIC (STAR) is a general-purpose detector providing precision particle identification and tracking [5]. It is presently the only active experiment at the RHIC. The STAR experiment has full azimuthal coverage over a wide range in rapidity as depicted in Fig. 2. The main detector upgrades for the BES-II included the installation of the inner Time Projection Chamber (iTPC), the endcap Time-of-Flight (eTOF) system, and the Event Plane Detector (EPD). These upgrades significantly increased the acceptance and tracking capabilities of the STAR experiment.

3. Collective Flow

Collective flow refers to the azimuthal anisotropy of produced particles with respect to the collision symmetry plane, which has been observed by relativistic heavy-ion collision experiments [6]. It can be quantified by the Fourier decomposition of the azimuthal angle distribution of produced particles with respect to the reaction plane angle (Ψ_n) [7],

$$E\frac{d^3N}{dp^3} = \frac{d^2N}{2\pi p_T dp_T d\eta} \times$$

$$\times \left(1 + 2\sum_{n=1}^{\infty} v_n \cos[n(\phi - \Psi_n)]\right), \quad (1)$$

where p_T, η, and ϕ are the particle transverse momentum, pseudorapidity, and the azimuthal angle, respectively. The Fourier coefficients v_n are commonly referred to as the flow coefficients. Specifically, the initial three coefficients are known as directed flow (v_1), elliptic flow (v_2), and triangular flow (v_3). These flow coefficients are extensively used to study the properties of the QGP.

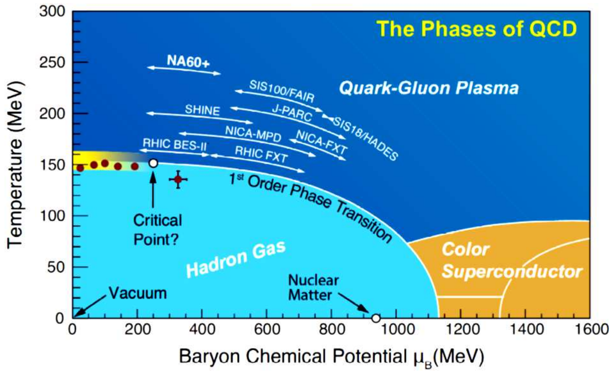

Fig. 1. Schematic layout of the QCD phase diagram [2]. The ranges (white arrows) shown are different experimental programs

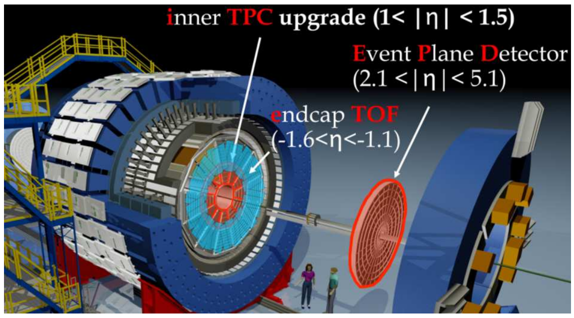

Fig. 2. The STAR experiment at RHIC with each of its subsystems and their associated acceptance

4. Results

4.1. Directed flow

The term "directed flow" (v_1) describes the collective sideward deflection of produced particles in the reaction plane and is believed to occur during the early stages of nuclear passage. Directed flow is quantified by the first-order flow coefficient v_1 in the azimuthal angle distribution of produced particles, measured relative to the first-order event plane.

In Fig. 3, the measured slope of v_1 is shown as a function of collision energy for various identified particles (a) and light and hyper nuclei (b) at mid-rapidity in mid-central Au + Au collisions from the

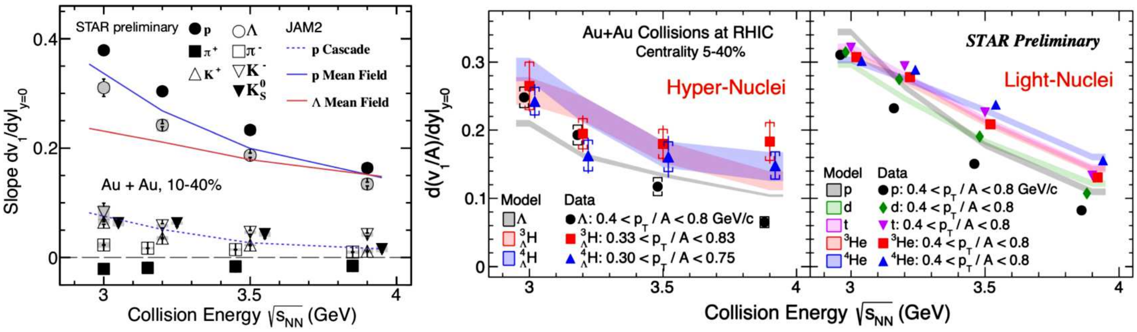

a *b*

Fig. 3. Slope of directed flow (dv_1/dy) for identified hadrons (a), $d(v_1/A)/dy$ for light and hyper nuclei (b), as a function of collision energy at mid-rapidity in Au + Au collisions from the STAR experiment at RHIC [8–10]

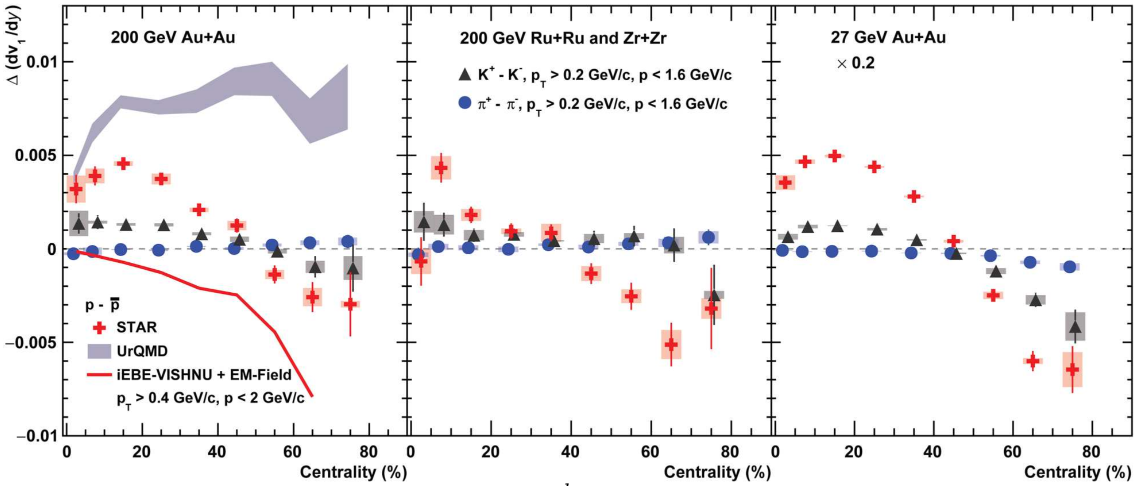

a *b* *c*

Fig. 4. The difference in the slope of directed flow ($dv_1(y)/dy$) as a function of centrality between particles and antiparticles in (a) Au + Au (b) Ru + Ru and Zr + Zr collisions at $\sqrt{s_{NN}} = 200$ GeV, and (c) in Au + Au collisions $\sqrt{s_{NN}} = 27$ GeV from the STAR experiment at RHIC [14]

FXT program of the STAR experiment at RHIC [8–10]. The slope at mid-rapidity for hadrons (p, K, and Λ) as well as for light and hyper nuclei decreases from $\sqrt{s_{NN}} = 3$ to 4 GeV. The Jet AA Microscopic (JAM) transport model [11] with momentum-dependent baryonic mean-field potential and incompressibility $k = 210$ MeV describes the measured v_1 slope for baryons compared to the cascade model, suggesting a strong mean-field at high baryon density region. The JAM model with coalescence is also consistent with $d(v_1/A)/dy$ for light and hyper nuclei, indicating coalescence as their particle production mechanism at high μ_{B}.

In relativistic heavy-ion collisions, nuclear fragments create a strong magnetic field expected to range from 10^{18} to 10^{19} Gauss [12]. When quarks, in presence of a QGP medium, interact with this field, they experience electromagnetic forces due to the Hall effect, Coulomb effect, and Faraday induction. This strong electromagnetic field can influence the collective flow of particles, leading to changes in flow coefficients from central to peripheral collisions. A positive $\Delta(dv_1/dy)$ is associated with transported quarks, while a negative $\Delta(dv_1/dy)$ is linked to the electromagnetic field [13]. As shown in Fig. 4, the observation of a negative $\Delta(dv_1/dy)$ in peripheral collisions supports the expected dominance of combined Faraday and Coulomb effect in these collisions [14]. A positive $\Delta(dv_1/dy)$ in (mid)central collisions for hadrons with non-transported constituent quarks can origi-

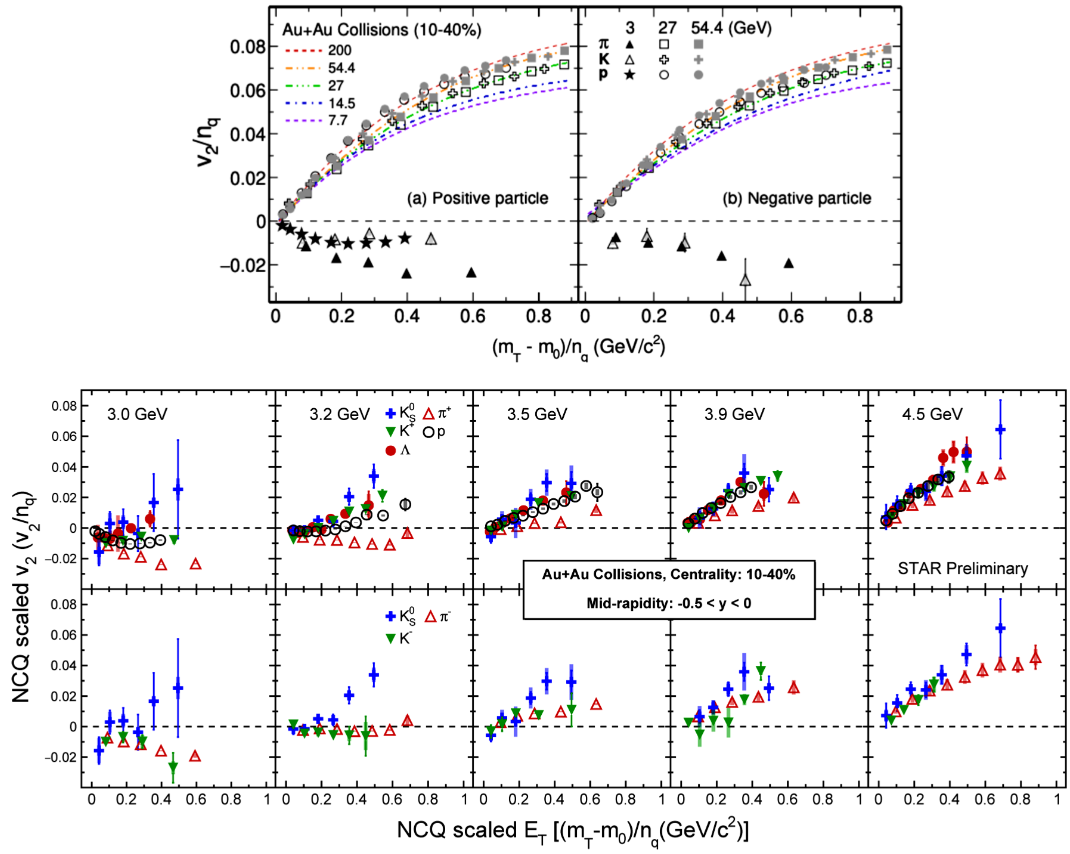

Fig. 5. NCQ scaled elliptic flow (v_2/n_q) as a function of NCQ scaled transverse kinetic energy $(m_T - m_0)/n_q$ for identified hadrons in 10–40% central Au + Au collisions from the STAR experiment at RHIC

nate from a dominance of hall effect [15]. Further investigations, including mean-field contributions, are ongoing to explore other mechanisms.

4.2. Elliptic flow

In non-central heavy-ion collisions, the initial overlap region is spatially anisotropic, resembling an elliptical almond shape. As a result of pressure gradients and multi-particle interactions among the constituents of the matter, the initial spatial anisotropy transforms into momentum space anisotropy in the final state. This can be quantified by the second-order flow coefficient v_2 in the azimuthal angle distribution of produced particles with respect to the event plane. The observation of a large positive v_2 and NCQ scaling of v_2 are consistent with the formation of a matter with partonic degrees of freedom at the RHIC and the LHC.

Figure 5 shows v_2 as a function of transverse kinetic energy scaled by number of constituent quarks for identified hadrons in 10–40% central Au + Au collisions from the STAR experiment at RHIC. A large positive v_2 and NCQ scaling is observed at $\sqrt{s_{NN}} =$ = 200 GeV down to 4.5 GeV, providing strong evidence for the formation of a QGP matter at the RHIC [8, 16, 17]. Below $\sqrt{s_{NN}} \leq 3.2$ GeV, the negative v_2 values and the violation of NCQ scaling, as shown in Fig. 5, and can originate from a transition from a medium dominated by partonic degrees of freedom to hadronic degrees of freedom.

4.3. Triangular Flow

An initial triangular shape in the initial geometry will result in a triangular flow v_3. This triangular shape, at higher energies, is attributed to event-by-event fluctuations in the positions of the participating

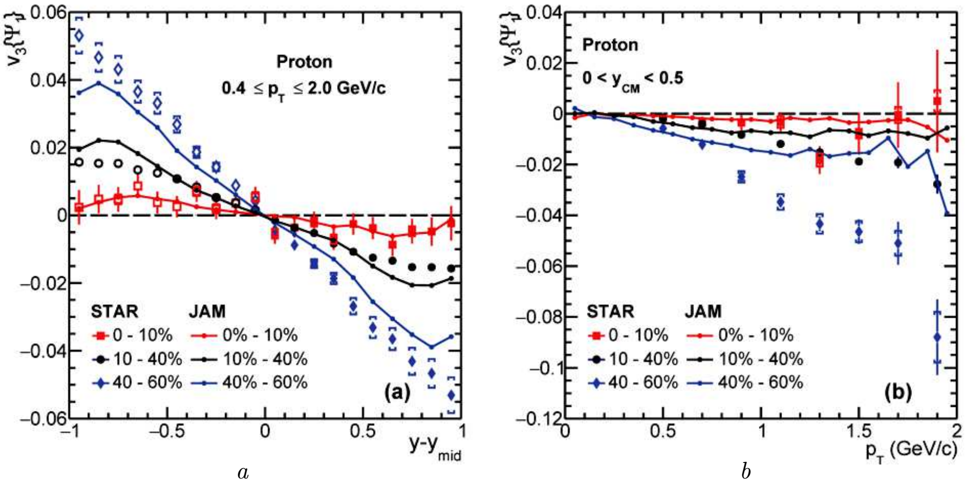

Fig. 6. Triangular flow $v_3\{\Psi_1\}$ as a function of rapidity (a) and p_T (b) for protons in Au + Au collisions at $\sqrt{s_{NN}} = 3$ GeV from the STAR experiment at RHIC [18]

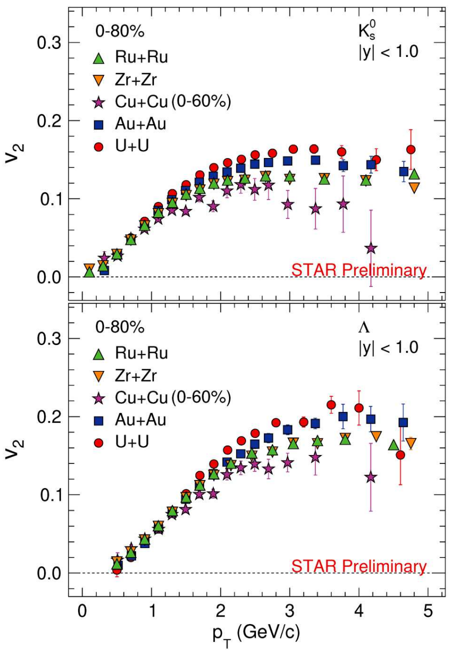

Fig. 7. Elliptic flow v_2 as a function of p_T for K^0_s and Λ at mid-rapidity ($|y| < 1.0$) in minimum bias U + U, Au + Au, Ru + Ru, Zr + Zr, and Cu + Cu collisions at $\sqrt{s_{NN}} = 200$ GeV from the STAR experiment at RHIC [16, 19, 20]

nucleons, and is uncorrelated to the initial reaction plane angle Ψ_1. At lower energies ($\sqrt{s_{NN}} = 3$ GeV) a triangular flow correlated to the reaction plane is clearly seen as shown in Fig. 6, indicating that the triangular shape arises from dynamical effects due to stopping, the passing time of the spectators and the expansion of the fireball. Figure 6 shows v_3 of protons measured with respect to the first order event plane angle Ψ_1 in Au + Au collisions at $\sqrt{s_{NN}} = 3$ GeV [18]. The values of $v_3\{\Psi_1\}$ show a negative slope as a function of rapidity, opposite to that of v_1 at this energy. Its magnitude is larger at higher rapidity, increases as one goes to higher p_T and towards more peripheral collisions. The JAM model [11] effectively describes the data, indicating that a momentum-dependent baryonic mean-field is crucial for the development of $v_3\{\Psi_1\}$ of protons in Au + Au collisions at $\sqrt{s_{NN}} = 3$ GeV, consistent with the conclusions drawn from v_1 and v_2 measurements at this energy.

4.4. Nuclear size and deformation

The STAR experiment at RHIC gathered data from a variety of collision systems, including U + U, Au + Au, and Cu + Cu at $\sqrt{s_{NN}} = 200$ GeV. In the year 2018, it collected data for isobar nuclei ($^{96}_{44}$Ru and $^{96}_{40}$Zr), which have the same atomic mass number but different atomic numbers and deformation parameters. Collective flow is highly sensitive to initial conditions, such as the initial overlap geometry, the size of the colliding nuclei, and their deformation. Additionally, studying the flow of strange hadrons can provide valuable insights into the initial state anisotropies due to their small hadronic interaction cross-section compared to light hadrons. There-

 ISSN 2071-0194. Ukr. J. Phys. 2024. Vol. 69, No. 11

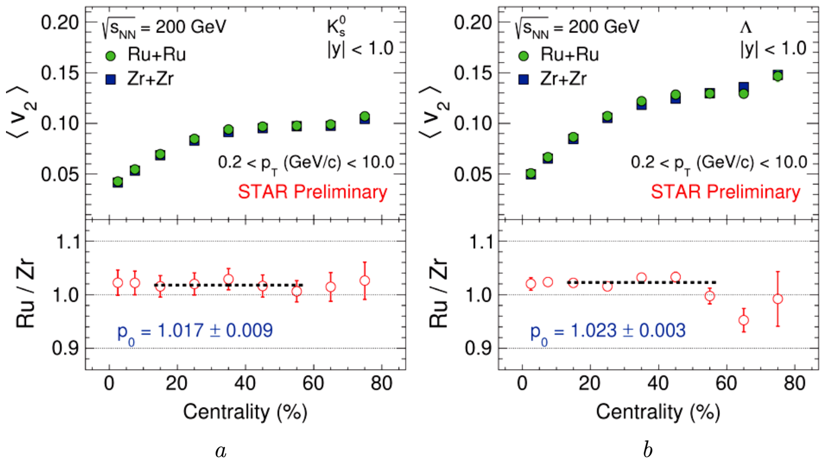

Fig. 8. Integrated elliptic flow ($\langle v_2 \rangle$) as a function centrality (%) for K_s^0 (a) and Λ (b) at mid-rapidity ($|y| < 1.0$) in Ru + Ru and Zr + Zr collisions at $\sqrt{s_{NN}} = 200$ GeV from the STAR experiment at RHIC. The bottom panels show ratio of $\langle v_2 \rangle$ between Ru and Zr, fitted with a constant polynomial function

fore, a systematic analysis of the anisotropic flow of strange hadrons helps understanding the impact of nuclear size and deformation in heavy-ion collisions.

Figure 7 shows $v_2(p_T)$ of strange hadrons (K_s^0 and Λ) at mid-rapidity ($|y| < 1.0$) in minimum bias U + U, Au + Au, Ru + Ru, Zr + Zr, and Cu + Cu at $\sqrt{s_{NN}} = 200$ GeV from the STAR experiment at RHIC [16, 19, 20]. The magnitude of v_2 for $p_T > 2.0$ GeV/c increases with the size of the colliding system, following the hierarchy $v_2^{\rm Cu} < v_2^{\rm Ru/Zr} < v_2^{\rm Au} < v_2^{\rm U}$, indicating a clear system size dependence of $v_2(p_T)$.

Figure 8 shows v_2 of strange hadrons integrated over $|y| < 1.0$ and $0.2 < p_T < 10$ GeV/c as a function of centrality in Ru + Ru and Zr + Zr collisions at $\sqrt{s_{NN}} = 200$ GeV. The ratio of v_2 in betwen Ru and Zr is also shown in the bottom panels and fitted with a constant polynomial function for mid-central collisions (20–50%). A deviation of ∼2% from unity with a significance of 6.25σ for Λ and 1.83σ for K_s^0 is observed, which is consistent with the expectation of the difference between the nuclear structures of the two isobar nuclei [21]. The correlations between flow harmonics and mean transverse momentum can also help understand nuclear deformation. Recent measurements have shown that, in central U + U collisions, the correlation coefficient $\rho(v_2^2, \delta p_T)$ changes from positive to negative values. This change suggests a significant deformation of the uranium nucleus compared to Au + Au collisions [22].

5. Summary

In summary, some selected experimental results on collective flow at the top RHIC energy ($\sqrt{s_{NN}} = 200$ GeV), BES-II program ($\sqrt{s_{NN}} = 3.0$ to 27 GeV) from the STAR experiment at RHIC are presented. These results include directed, elliptic, and triangular flows of identified hadrons, light, and hypernuclei. The possible relations of the results to the formation of the QGP medium, Parton-hadron phase transition in the QCD phase diagram, and nuclear geometry are discussed. The observed slope of v_1 is described by the hadronic transport JAM model, which incorporates a momentum-dependent baryonic mean-field potential. This suggests a strong mean-field effect at high $\mu_{\rm B}$. Furthermore, light and hyper nuclei $d(v_1/A)/dy$ is consistent with the JAM model with coalescence, indicating coalescence as their particle production mechanism at high $\mu_{\rm B}$. Absence of NCQ scaling of v_2 at $\sqrt{s_{NN}} = 3$ and 3.2 GeV indicates baryonic interactions dominate the nuclear EoS. Results for charge-dependent v_1 indicate the dominance of the Faraday and Coulomb effect in peripheral collisions. Moreover, findings from the data collected on deformed nuclei, including Isobars (Ru + Ru and Zr + Zr) and U + U collisions, indicate that it is possible to explore nuclear structure in high-energy heavy-ion collisions. Finally, STAR has completed a forward upgrade [23] targeted for the RHIC runs from 2022–2025 with $p+p$, $Au+Au$ and $p+Au$ collisions data and will be ready to analyze in future years.

1. D.J. Gross, R.D. Pisarski, L.G. Yaffe. QCD and instantons at finite temperature. *Rev. Mod. Phys.* **53**, 43 (1981).
2. A.D. Falco (for the NA60+ Collaboration). Prospects for the NA60+ experiment at the CERN SPS. *EPJ Web Conf.* **259**, 09003 (2022).
3. A. Bazavov *et al.* Chiral crossover in QCD at zero and non-zero chemical potentials, *Phys. Lett. B* **795**, 15 (2019).
4. The STAR Collaboration. Studying the phase diagram of QCD matter at RHIC. *Star Note* **0598** (2014).
5. K.H. Ackermann *et al.* (STAR Collaboration). STAR detector overview. *Nucl. Instrum. Meth. A* **499**, 624 (2003).
6. S.A. Voloshin, A.M. Poskanzer, R. Snellings. Collective phenomena in non-central nuclear collisions. *Landolt–Bornstein* **23**, 293 (2010).
7. A.M. Poskanzer, S.A. Voloshin. Methods for analyzing anisotropic flow in relativistic nuclear collisions. *Phys. Rev. C* **58**, 1671 (1998).
8. M.S. Abdallah *et al.* (STAR Collaboration). Disappearance of partonic collectivity in $\sqrt{s_{NN}} = 3$ GeV $Au+Au$ collisions at RHIC, *Phys. Lett. B* **827**, 137003 (2022).
9. M.S. Abdallah *et al.* (STAR Collaboration). Light nuclei collectivity from $\sqrt{s_{NN}} = 3$ GeV $Au+Au$ collisions at RHIC. *Phys. Lett. B* **827**, 136941 (2022).
10. B.E. Aboona *et al.* (STAR Collaboration). Observation of directed flow of hypernuclei ${}^{3}_{\Lambda}H$ and ${}^{4}_{\Lambda}H$ in $\sqrt{s_{NN}} = 3$ GeV $Au+Au$ collisions at RHIC. *Phys. Rev. Lett.* **130**, 212301 (2023).
11. Y. Nara, A. Ohnishi. Mean-field update in the JAM microscopic transport model: Mean-field effects on collective flow in high-energy heavy-ion collisions at $\sqrt{s_{NN}} = 2$–20 GeV energies. *Phys. Rev. C* **105**, 014911 (2022).
12. U. Gürsoy *et al.* Charge-dependent flow induced by magnetic and electric fields in heavy ion collisions. *Phys. Rev. C* **98**, 055201 (2018).
13. P. Bozek. Splitting of proton-antiproton directed flow in relativistic heavy-ion collisions, *Phys. Rev. C* **106**, L061901 (2022).
14. M.I. Abdulhamid *et al.* (STAR Collaboration). Observation of the electromagnetic field effect via charge-dependent directed flow in heavy-ion collisions at the relativistic heavy ion collider. *Phys. Rev. X* **14**, 011028 (2024).
15. The STAR Collaboration. Electric charge and strangeness-dependent directed flow splitting of produced quarks in $Au+Au$ collisions, *arXiv:2304.02831 [nucl-ex]* (2023).
16. B.I. Abelev *et al.* (STAR Collaboration). Centrality dependence of charged hadron and strange hadron elliptic flow from $\sqrt{s_{NN}} = 200$ GeV $Au+Au$ collisions. *Phys. Rev. C* **77**, 054901 (2008).
17. L. Adamczyk *et al.* (STAR Collaboration). Centrality dependence of identified particle elliptic flow in relativistic heavy ion collisions at $\sqrt{s_{NN}} = 7.7$–62.4 GeV. *Phys. Rev. C* **93**, 014907 (2016).
18. M.I. Abdulhamid *et al.* (STAR Collaboration). Reaction plane correlated triangular flow in $Au+Au$ collisions at $\sqrt{s_{NN}} = 3$ GeV. *Phys. Rev. C* **109**, 044914 (2024).
19. B.I. Abelev *et al.* (STAR Collaboration). Charged and strange hadron elliptic flow in $Cu+Cu$ collisions at $\sqrt{s_{NN}} = 62.4$ and 200 GeV. *Phys. Rev. C* **81**, 044902 (2010).
20. M.S. Abdallah *et al.* (STAR Collaboration). Azimuthal anisotropy measurements of strange and multistrange hadrons in $U+U$ collisions at $\sqrt{s_{NN}} = 193$ GeV at the BNL Relativistic Heavy Ion Collider. *Phys. Rev. C* **103**, 064907 (2021).
21. P. Sinha *et al.* Effect of nuclear structure on particle production in relativistic heavy-ion collisions using a multiphase transport model. *Phys. Rev. C* **108**, 024911 (2023).
22. STAR Collaboration. Imaging shapes of atomic nuclei in high-energy nuclear collisions. *arXiv:*2401.06625 (2024).
23. J.D. Brandenburg *et al.* The STAR Forward Silicon Tracker. *arXiv:*2407.09952 (2024).

Received 07.10.24

В. Байраті (від імені колаборації STAR)

КОЛЕКТИВНІ ВЛАСТИВОСТІ
ЯДЕРНОЇ МАТЕРІЇ З ЕКСПЕРИМЕНТУ
В РАМКАХ STAR НА КОЛАЙДЕРІ RHIC

Дослідження колективного потоку дає цінну інформацію про динаміку та властивості кварк-ґлюонної плазми (КҐП), що утворюється у зіткненнях важких йонів. Очікується, що для спрямованого потоку (v_1) у випадку протонів середньої хуткості, нахил (dv_1/dy) буде чутливим до фазового переходу першого роду. Скейлінг еліптичного потоку (v_2) за кількістю складових кварків можна розглядати як ознаку формування КҐП. Трикутний потік (v_3) зазвичай виникає внаслідок флуктуацій і може накладати обмеження на геометрію початкового стану та флуктуації. За допомогою детектора STAR на колайдері RHIC зібрано експериментальні дані для широкого діапазону енергій і систем. Другий етап програми Beam Energy Scan, включаючи режим Fixed-Target, виконується для збору даних про зіткнення $Au+Au$ із значною статистикою в області великої густини баріонів на фазовій діаграмі квантової хромодинаміки (КХД). У цій статті ми обговорюємо деякі результати, отримані для колективних властивостей ядерної матерії з експериментів за допомогою детектора STAR на колайдері RHIC.

Ключові слова: зіткнення важких йонів, кварк-ґлюонна плазма, колективний потік.